Pakistan Veterinary Journal

ISSN: 0253-8318 (PRINT), 2074-7764 (ONLINE)
DOI: 10.29261/pakvetj/2026.040

RESEARCH ARTICLE

Mangiferin Enhances the Anticancer Efficacy of Paclitaxel by Targeting Apoptosis, Autophagy, and Angiogenesis

Ayca Uvez[1], Engin Ulukaya[2] and Elif Ilkay Armutak*[1]

[1]Department of Histology and Embryology, Faculty of Veterinary Medicine, Istanbul University- Cerrahpasa, Istanbul-Turkey; [2]Department of Clinical Biochemistry, Faculty of Medicine, Istinye University, Istanbul- Turkey
*Corresponding author: elif@iuc.edu.tr

ARTICLE HISTORY (25-323)

Received: April 14, 2025
Revised: March 01, 2026
Accepted: March 08, 2026
Published online: March 09, 2026

Key words:
Antiangiogenic effect
Apoptosis
Autophagy
breast cancer
Mangiferin
Paclitaxel

ABSTRACT

Despite advances in cancer therapy, conventional treatment modalities often remain insufficient in achieving optimal outcomes. To address these limitations, growing attention has been directed toward combining chemotherapeutic agents with natural compounds. The present study investigates the effects of co-treatment with mangiferin and paclitaxel on key cancer-related biological processes, including proliferation, apoptosis, autophagy, and angiogenesis. The cytotoxicity was assessed using the ATP assay on Ehrlich ascites carcinoma (EAC) and HUVECs. Protein expression in EAC cells was analyzed by western blotting. In vivo, tumor growth, cell death, and autophagic activity were examined in EAC tumors. Angiogenic responses were examined using *In vitro* tube formation and an *In vivo* chorioallantoic membrane assay. The combined treatment resulted in a synergistic cytotoxic effects. Increased LC3B and decreased p62, along with the induction of FAS and cleaved PARP, suggest involvement of both apoptosis and autophagy. *In vitro* results were consistent with *in vivo*. Mangiferin (50mg/kg) combined with paclitaxel showed the greatest tumor reduction with concurrent induction of apoptosis and autophagy. Furthermore, the co-treatment exhibited stronger anti-angiogenic effect than either compound alone. In conclusion, mangiferin enhances the anticancer efficacy of paclitaxel by simultaneously targeting proliferation, programmed cell death, and angiogenesis. This supports the use of mangiferin as a promising natural agent for novel cancer treatment strategies.

To Cite This Article: Uvez A, Ulukaya E and Armutak EI, 2026. Mangiferin enhances the anticancer efficacy of paclitaxel by targeting apoptosis, autophagy, and angiogenesis. Pak Vet J, 46(3): 503-517. http://dx.doi.org/10.29261/pakvetj/2026.040

INTRODUCTION

Natural compounds are increasingly explored for treating life-threatening diseases. Recent studies have combined natural compounds with chemotherapeutic agents to increase their efficacy and reduce side effects (J. Wu *et al.*, 2023). Mangiferin (MNG) is a xanthone derivative mainly obtained from Mangifera indica. It is also present in various parts of species belonging to 16 different families, including Gentianaceae, Anacardiaceae, and Iridaceae (Dutta *et al.*, 2023). MNG has high therapeutic potential due to its phenolic groups and structural features, including C-glycoside and polyhydroxy groups (Rodriguez-Gonzalez *et al.*, 2021). MNG exhibits diverse pharmacological activities, including analgesic, antidiabetic, anti-sclerotic, antimicrobial, antiviral, and antiallergic effects. It also has protective effects on the heart, liver, and nervous system (Mei *et al.*, 2021). Several studies have focused on the essential role of MNG in cancer treatment (Yap *et al.*, 2021; Irshad *et al.*, 2024). MNG effectively suppresses cell growth, proliferation, migration, and invasion and induces apoptosis in breast cancer cells. *In vivo* studies further confirm that MNG suppresses tumor growth in breast cancer xenografts (B. Wang *et al.*, 2018; Yap *et al.*, 2021). The anticancer properties of MNG are attributed to multiple mechanisms, including the downregulation of inflammation, inhibition of the cell cycle, protection against oxidative stress and DNA damage, and enhancement of apoptosis (Aboyewa *et al.*, 2021). Some studies also show that MNG is a valuable agent for enhancing the anticancer activity of chemotherapeutic agents. Several studies have focused on the synergistic interactions of MNG with platinum based drugs and doxorubicin. He *et al.* (2018) reported that MNG inhibits tumor cell growth and enhances cisplatin sensitivity (He *et al.*, 2018). Another study showed that MNG improved the efficacy of oxaliplatin by increasing apoptotic cell death while reducing the resistance to this

chemotherapy (du Plessis-Stoman *et al.*, 2011). Paclitaxel (PTX) is widely used to treat many types of cancer (Jiang, 2025). However, to date, there are no reports about the effects of the combination of MNG and paclitaxel on proliferation, apoptosis, autophagy, survival, and angiogenesis.

The present study aims to investigate the effects of MNG, PTX, and their combinations on proliferation, apoptosis, autophagy, survival, and angiogenesis. A comprehensive evaluation of the mechanisms was conducted through a combination of in vitro experiments utilizing Ehrlich ascites carcinoma (EAC) cells and human umbilical vein endothelial cells (HUVECs), complemented by in vivo studies in EAC-inoculated mice.

MATERIALS AND METHODS

Chemicals and Cell Lines: Mangiferin was purchased from Sigma-Aldrich Co., and Paclitaxel was obtained from Bristol Myers Squibb. EAC cells were sourced from the Aziz Sancar Institute of Experimental Medicine at Istanbul University, while Human umbilical vein endothelial cells (HUVECs) were acquired from the American Type Culture Collection (ATCC). EAC cells were cultured in RPMI medium supplemented with 100U/mL penicillin, 100µg/mL streptomycin, 2mM L-glutamine, and 5% fetal bovine serum at 37°C in a humidified atmosphere with 5% CO^2. HUVECs were cultured in Endothelial Cell Growth Medium-2 (EGM-2) BulletKit (Lonza, Switzerland) in a humidified environment at 37°C and 5% CO2.

In vitro assays

Cytotoxicity assay: Drug-induced cytotoxicity was determined by the ATP viability assay (ATP Bioluminescent Somatic Cell Assay Kit; Sigma). 5×10^3 EAC cells and HUVECs were seeded per well of 96-well plates and incubated overnight. Briefly, after 24 hours, cells were treated with MNG (6.25-300µM) and PTX (0.25-15.9µM) alone and in combination for 48 hours. Intracellular ATP was extracted from the cells, and measurements were performed as in our previous study (Uvez *et al.*, 2020).

Western blotting: Western blotting was performed as described in previous studies (Aydinlik *et al.*, 2021). Cells were treated with PTX 3.98µM, MNG 300µM, and their combination for 48h. Protein (30µg) was subjected to 8-12% SDS-PAGE, then transferred to a nitrocellulose membrane. Primary antibodies used were anti-PARP-1 (#9532), anti-Fas (#4233), anti-DR4 (#42533), anti-Bax (#2772), anti-PTEN (#9552), anti-p-SRC (#2101), anti-p-AKT (#9271), anti- p-c-jun (#3270), anti-Beclin-1 (#84966), anti-Atg5 (#12994), anti-LC3A (#4599), anti-LC3B (#3868) (1:1000 dilution; Cell Signaling Technology), mouse anti-p62/SQSTM1 (2C11, Abnova, Taiwan), and rabbit anti-β-actin monoclonal antibody (1:1000 dilution; Cell Signaling Technology). Secondary antibodies conjugated with HRP (1:2000; Cell Signaling Technology) were used. EMD Millipore Luminata Forte Western HRP substrate was used to detect the primary antibodies. Bands were visualized using a Fusion FX-7 imaging device (VilberLourmat, France).

Tube formation assay: The tube formation assay was performed using HUVEC, as described in our previous study (Uvez *et al.*, 2020). Briefly, each well was coated with 50µL/ per Matrigel in 96-well plates (BD Biosciences, USA). HUVECs (1.5×10^4 cells/well) were suspended in a low serum (1%) culture medium containing either MNG (12.5- 50µM) or Paclitaxel (1.99- 15.93µM) alone or in combination and were then seeded. Thalidomide and DMSO were used as positive and negative controls. Tube structures were evaluated after 4, 8, 12, and 16h under an inverted microscope.

In vivo assays

***In vivo* experimental design:** The EAC cells exhibit characteristics that closely mimic the behavior of human breast cancer cells, which is crucial for studying the progression of the disease and evaluating potential treatments (Radulski *et al.*, 2023). The *in vivo* solid tumor model protocol was approved by the Animal Welfare and Use Committee of Istanbul University (No: 141199/12.04.2017). Seventy-eight Balb-c mice (approximately 24±2g) were subcutaneously injected with 2.5×10^6 EAC cells in serum free medium to induce solid carcinoma (Ikitimur-Armutak *et al.*, 2015) (day 1), and then they were randomly divided into eight groups: the control group (n=8) and seven experimental groups (n=10; MNG 25mg/kg, MNG 50mg/kg, MNG 100mg/kg, PTX 12.5mg/kg, MNG 25mg/kg +PTX 12.5mg/kg, MNG 50 mg/kg + PTX 12.5 mg/kg, and MNG 100mg/kg + PTX 12.5mg/kg). MNG at the indicated doses was administered orally until day 12, either alone or in combination with PTX. PTX at 12.5 mg/kg (Bristol Myers Squibb) was administered subcutaneously alone or in combination with MNG on the 5^{th} and 12^{th} experimental days. On the 14^{th} day, mice were humanely euthanized by cervical dislocation, and all tumors were excised and measured with a caliper. The tumor volume was calculated by the following formula: V(mm3)=a × b2/2, where V(mm3) is the tumor volume in mm3, a=length, and b=width of the tumors (Ikitimur-Armutak *et al.*, 2015). Subsequently, all tumor tissues were rapidly fixed in 4% formaldehyde solution and subsequently embedded in paraffin.

Immunohistochemical Analysis: 4µm-thick sections were collected onto positively charged slides, and then the sections were deparaffinized and rehydrated. Antigen retrieval, endogenous peroxidase, and protein blocking procedures were performed (Ikitimur-Armutak *et al.*, 2015). PCNA (1:100, SC56, Santa Cruz Biotechnology), cleaved PARP (1:100 AB91526 Abcam), AKT (1:150 NBP1-69923, Novus Biologicals), PTEN (1:100, NB100-92219, Novus Biologicals), ATG5 (1:300, #9271, Cell Signaling), and p62 (1:300, ab91526, Abcam) were incubated overnight at 4˚C. LC3-A (1:750, #4599, Cell Signaling), LC3-B (1:750, #3868, Cell Signaling), and cleaved (active) caspase-3 (1:1500, NB100-56113, Novus Biologicals) were incubated for 1.5h at room temperature. A commercial secondary antibody kit (TP-125-BN, and TS-125-HR, Thermo Scientific) was used following the manufacturer's instructions. Proteins were visualized with an AEC (3-amino-9-ethyl carbazole) substrate kit (TA-004-HAC, Thermo Scientific). Mayer's hematoxylin was used for counterstaining.

Detection of apoptosis by DNA fragmentation assay (TUNEL): Apoptosis was assessed using a commercial TUNEL kit (S7101, MILLIPORE,) according to the manufacturer's instructions (Ikitimur-Armutak *et al.*, 2015).

Assessment of immunohistochemistry and TUNEL assay: Immunohistochemical staining was quantified for further evaluation using a histologic score (H-Score) and index (Adiyeke *et al.*, 2024) for BAX, AKT, PTEN, LC3-A, LC3B, ATG5, and p62. The H-score value was calculated with the following formula: "H-Score= Pi (i+1)", where "i" is the intensity score and "Pi" is the percentage of cells with the same intensity scores. Staining was determined as "0, no staining; 1, weak staining; 2, moderate or distinct staining; 3, intense staining". Proliferative (PCNA) and apoptotic (cleaved PARP, active (cleaved) caspase 3, and TUNEL) index (percentage of positive cells in 800-1000 cells) was calculated with the following formula: "100 × (positive cell number/total cell number)" (Ikitimur-Armutak *et al.*, 2015). Sections were examined by two different observers at a 40× magnification.

Chick Chorioallantoic Membrane (CAM) Assay: The in vivo CAM assay was conducted as described previously by our research group (Uvez *et al.*, 2020; Üvez *et al.*, 2021). All studies were performed on fertilized chicken eggs at 36.5°C and a relative humidity of 80% for a 7-day incubation time. The CAM assay groups were as follows: 5mg/mL, 2.5mg/mL, and 1.25mg/mL concentrations of MNG; 0.3mg/mL, 0.15mg/mL, 0.075mg/mL, and 0.0375mg/mL concentrations of PTX and their combinations. (±)Thalidomide (5mg/mL) was used as a positive control. All samples were dissolved in a 2.5%(w/v) agarose (UltraPure, Invitrogen) solution. Drug pellets (10µL) were prepared and rapidly applied to the CAM. Forty-five eggs were used for each test group. The antiangiogenic effect on capillaries was briefly evaluated under the stereo-microscope with Leica Application Suite, Las V4.7. Antiangiogenic effects were quantified using formula 1 and scored according to Table 1(Krenn *et al.*, 2009).

Table 1. Semi quantitative scoring system for evaluating antiangiogenic effects on CAM

Score	Antiangiogenic effect	Effects observed on CAM after treatment
<0.5	Inactive	No change (Normal embryo growth).
0.5-0.75	Weak	No capillary free area. Area with reduced density of capillaries around the pellet not larger than its own area.
>0.75-1	Strong	Small capillary free area or area with significantly reduced density of capillaries. Effects not larger than double the size of the pellet.
>1	Very strong	Capillary free area around the pellet at least doubles the size of the pellet.

$$Average\ score = [Number\ of\ eggs\ (score > 1) \times 2 + Number\ of\ eggs\ (score > 0.75 - 1) \times 1] \div (Total\ number\ of\ eggs\ scored)$$

Statistical analysis: Statistical analyses were performed using GraphPad Prism 6.0 statistical software for Windows. At least three independent experiments were performed for all in vitro studies. The significance was determined using a one-way analysis of variance (ANOVA) was followed by Tukey's post hoc test for H-Score, Index, and CAM assays, and by Dunnett's test for other comparisons. All results were expressed as mean ± SD. Levels of *P<0.05 were considered statistically significant.

RESULTS

Evaluation of *In vitro* studies

Cytotoxic effects of Paclitaxel, Mangiferin, and their combinations on EAC cells and HUVECs: Cytotoxic effects of MNG (6.25µM-300µM), PTX (0.25µM-15.9µM), and their combination were evaluated on EAC cells and HUVECs by the ATP viability assay, as shown in Fig. 1A. MNG alone was found not to be cytotoxic against EAC cells and HUVECs after 48h of treatment. On the other hand, PTX showed dose-dependent cytotoxic effects in both cell lines. Cell viability of EAC cells was found to decrease more than 50% at a dose of 7.97µM PTX (P<0.001). When 200µM and 300µM of MNG were combined with increasing doses of PTX in EAC cells, cell viability decreased in a dose-dependent manner (Fig. 1A, P<0.01; P<0.001). When the viability of HUVECs was evaluated with combinations of the two agents, it was found that with increasing doses of PTX, the concentration of MNG 6.25µM-100 µM showed a dose-dependent cytotoxic effect, as shown in Fig. 1B (P<0.001). The combination of MNG 12.5µM with PTX 3.98-7.97-15.9µM produced the greatest reduction in HUVEC viability (P<0.001). The results show that MNG synergizes with PTX and exhibits a dose-dependent cytotoxic effect on HUVECs (Fig. 1B).

In vitro evaluation of apoptosis, autophagy, and survival: Apoptotic effects of PTX (3.98µM), MNG (300µM), and their combination on EAC cells were assessed 48 h post-treatment by western blot of DR4, FAS, BAX, and cleaved PARP-1 (Fig. 2). No difference was observed in DR4 expression. However, in the combination group, FAS expression increased approximately two-fold compared to the control group. On the contrary, BAX expression decreased by more than half of the control in the combination group. Additionally, we observed that cleaved PARP-1 was increased in the combination group. Phosphorylated Beclin (p-Beclin) as an early autophagy marker, Atg5, LC3A, and LC3B as autophagosome markers, and P62 as an autophagy cargo protein were also examined, as shown in Fig. 2. The combination group observed an eight-fold increase in p-Beclin expression compared to the controls. Atg5 levels were decreased in all treatments, while no obvious change in the LC3A expression was observed in any of the treatment groups. On the contrary, the LC3B expression was two times higher in the combination group than in the control. The p62 protein expression showed a decrease in the combination groups. To further evaluate the effect of these drugs on intracellular signaling pathways, the expression of p-SRC, p-AKT, PTEN, and p-c-Jun proteins was examined, as shown in Fig. 2. The expression of p-SRC showed an increase in the combination group, while p-c-Jun expression was significantly decreased in the same group compared with the control. No changes were observed in the expression of p-AKT and PTEN, as shown in Fig. 2.

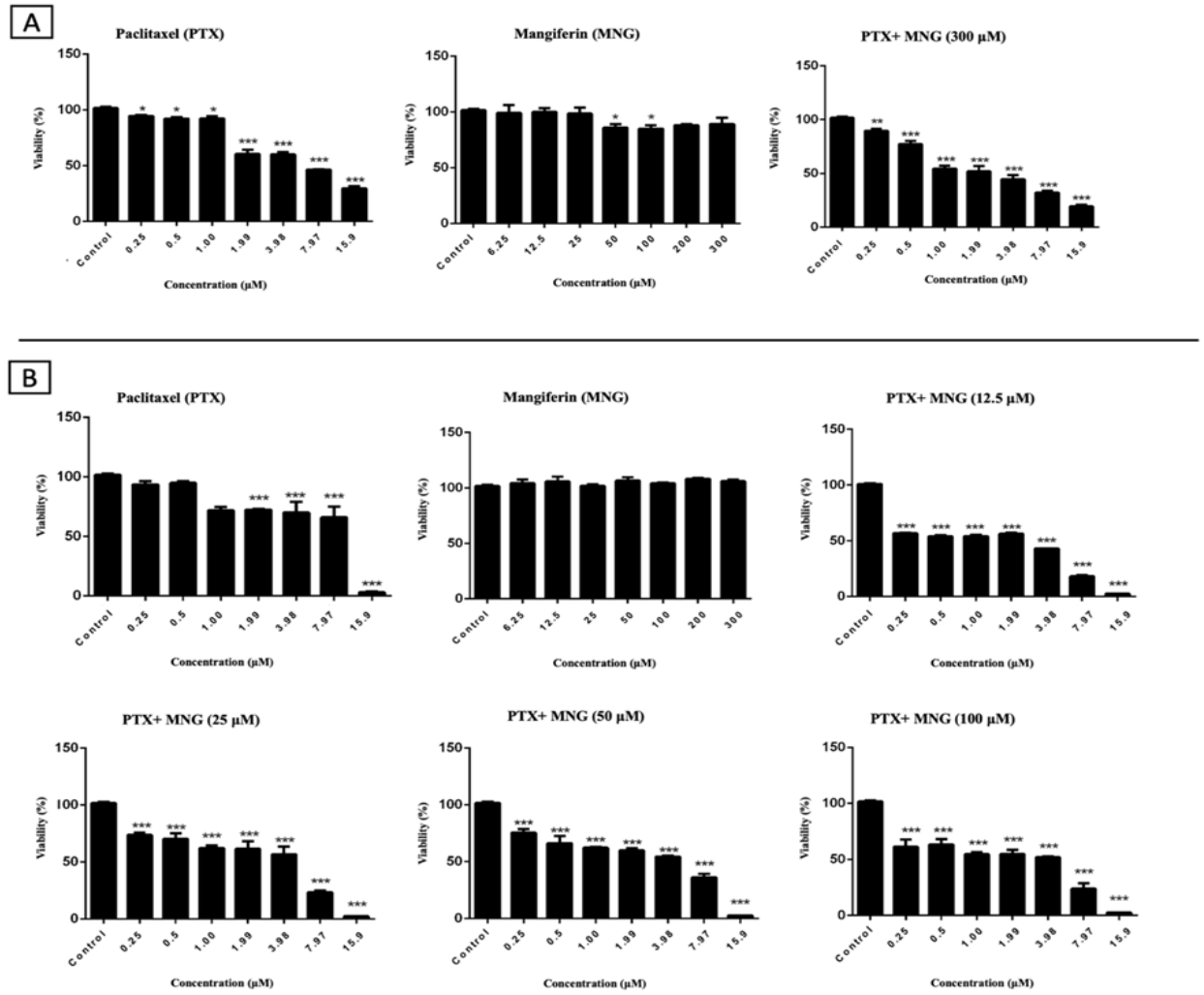

Fig. 1. A) The growth inhibitory effect of combined treatment with PTX and MNG on the Ehrlich ascites carcinoma (EAC) cell line was measured after 48 hours of treatment using the ATP assay. EAC cells were treated with MNG (0-300µM), PTX (0-15.9µM) and combinations of MNG 300µM and increasing PTX doses (0-15.9µM). The cell viability (%) of drug-treated cells is shown in graphs. **B)** The anti-growth effects of combinatorial treatment with PTX, MNG, and their combination on human umbilical vein endothelial (HUVEC) cells were measured using the ATP assay after 48 h treatment. HUVECs were treated with MNG (0 - 300µM), PTX (0 - 15.9µM), and combinations of MNG (12.5-25-50-100µM) and increasing doses of PTX (0 - 15.9µM). The cell viability (%) of drug-treated cells is shown in graphs. Bars represent the average±standard error of the mean (SEM). Statistically significant different at: *P<0.05, **P<0.01 and ***P<0.001.

***In vitro* evaluation of angiogenesis via tube formation assay on HUVECs:** MNG was found to effectively suppress the tube formation of HUVECs at a concentration of 50µM after 16 hours of treatment, as shown in Fig. 3. PTX slightly reduced tube formation at a concentration of 1.99µM but significantly blocked tube formation and showed a stronger disruptive effect on tubes than the positive control thalidomide at higher doses, as shown in Fig. 3. 12.5µM of MNG with 0.5 µM-15.93µM of PTX exhibited mild blocking effects on tube formation in all combinations. Combinations of ineffective doses of PTX (0.5µM, 1µM, and 1.99µM) and MNG had a strong blocking effect on tube structure, similar to the higher doses of PTX. Overall, the combination of MNG and PTX has a stronger disrupting effect on tube formation than the positive control thalidomide, as shown in Fig. 3.

Evaluation of *in vivo* experimental studies

Mangiferin or paclitaxel alone or in combination suppressed EAC solid tumor growth.: EAC tumor volumes were significantly reduced in all treated groups of mice compared to the control, as shown in Fig. 4A. The individual treatments with MNG (at 25, 50, and 100mg/kg) showed similar significant decreases in tumor size (P<0.001). Also, compared to control, tumor volumes decreased significantly in the group treated with 12.5 mg/kg of PTX (P<0.01). In the combination groups, a significant decrease in tumor volume was observed when PTX was combined with MNG at 25 and 50mg/kg (P<0.001). Interestingly, no synergistic effect was shown in the MNG 100mg/kg and PTX combination group compared to single treatment with MNG 100mg/kg. (Fig. 4A).

Mangiferin, paclitaxel, and their combinations decreased the cell proliferation of EAC cells in solid tumors: In all treated groups, a significant decrease was observed in the PCNA index compared with the control, as shown in Fig. 4A-B (P<0.001). The most significant decrease was also observed in the group that received a combination of 50 mg/kg of MNG + PTX at 12.5mg/kg compared with the control (P<0.001). However, similar to the tumor volume results, MNG 100mg/kg did not show synergistic effects with PTX, as the decrease of PCNA indices was the same as in single treatments (Fig. 4).

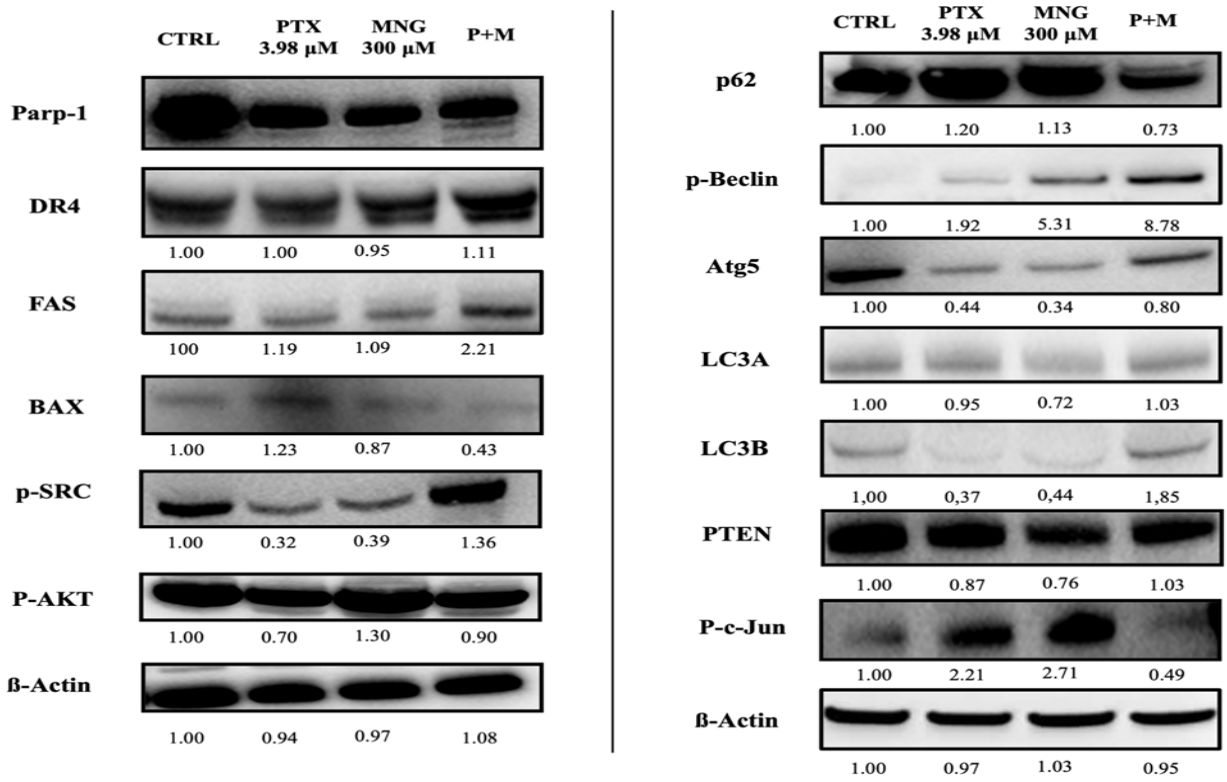

Fig. 2. PTX, MNG and their combination effects on apoptosis, autophagy, and survival pathway was investigated by western blotting. PTX (at 3.98µM), MNG (at 300µM) and their combination on EAC cells, western blot analysis was performed 48 hours after treatment. Expressions of apoptotic (DR4, FAS, BAX and cleaved PARP-1), autophagy (p-Beclin, Atg5, LC3A, LC3B and P62) and intracellular signaling (p-SRC, p-AKT, PTEN and p-c-Jun) pathway proteins were shown. Beta-actin was used as a housekeeping gene. Densitometry was performed using ImageJ software and the intensity of the observed bands was normalized to β-actin and quantified relative to controls set to 1.0.

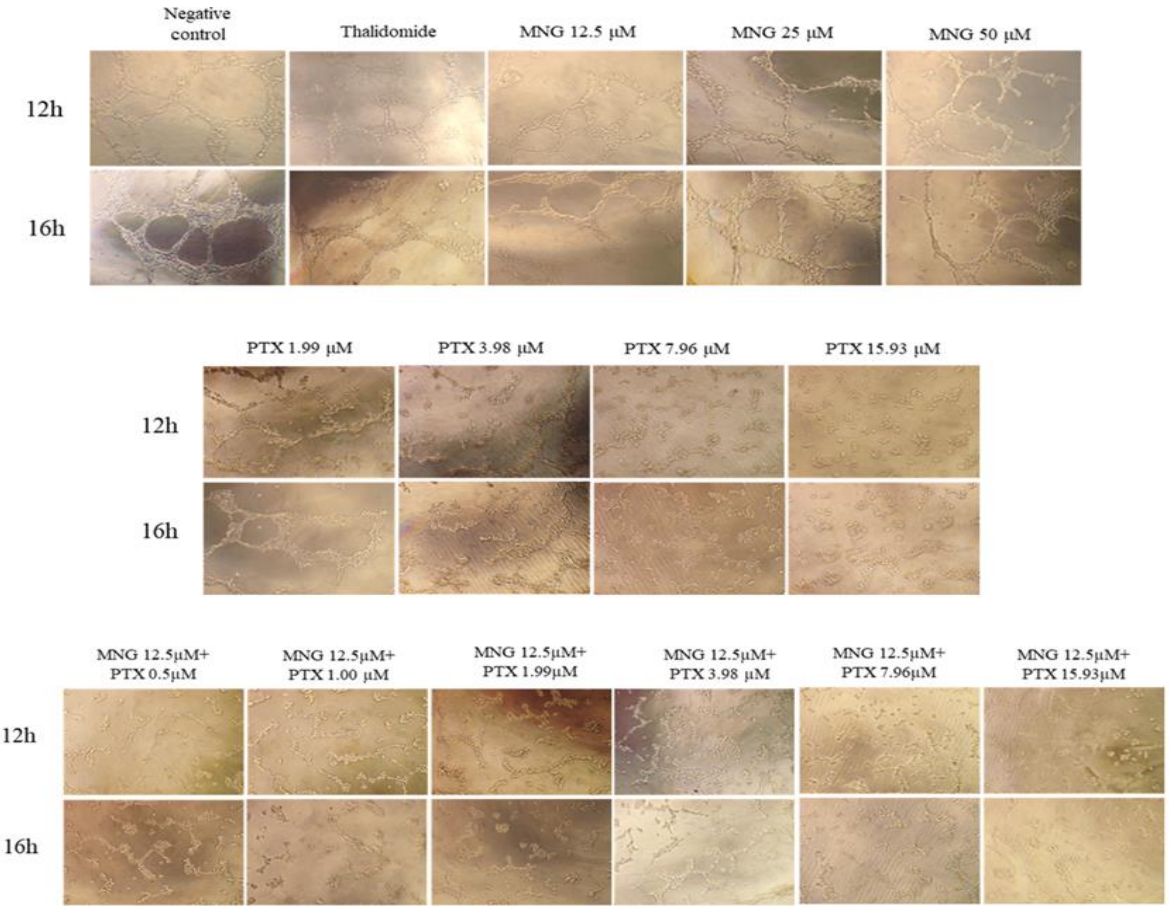

Fig. 3: Disturbing effect of MNG, PTX, and their combinations on tubes.In vitro antiangiogenic effects of negative and positive (Thalidomide 200µM) controls, MNG (12.5µM, 25µM and 50µM), PTX (1.99 -15.93µM) and MNG 12.5 µM and PTX (0.5 -15.93µM) combinations were shown in HUVECs at 0-16h.

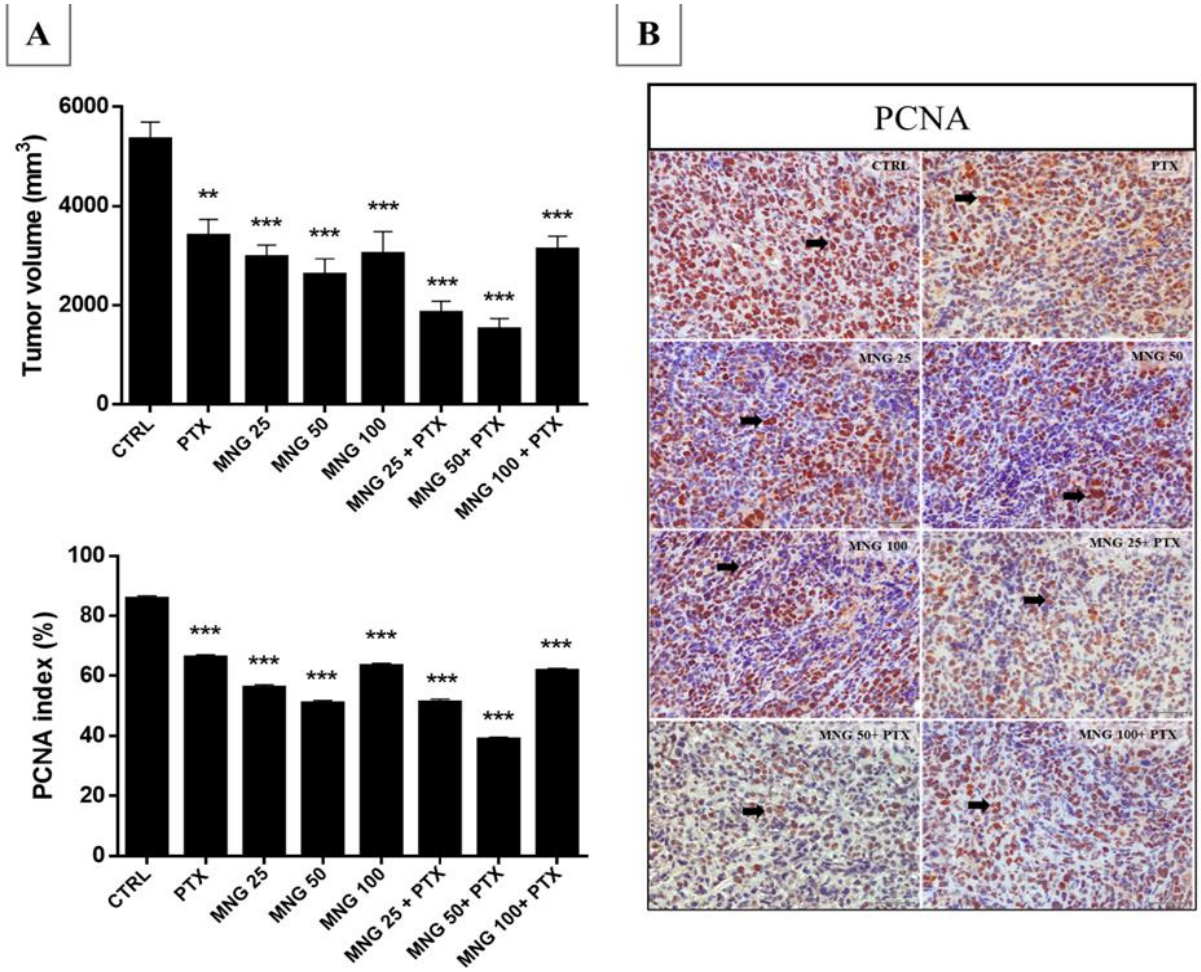

Fig. 4: A) Tumor volume (mm3), PCNA index (%) results and **B)** Immunohistochemical micrograph of PCNA. EAC carcinoma tumors treated with PTX (12.5mg/kg), MNG (25-50-100mg/kg) and their combination. Immunoreactivity is nuclear and red-brown. Proliferative cells are shown with an arrow (→) . **P<0.01 and ***P<0.001, significance compared to the control group. Scale bars = 50μM (× 400).

Mangiferin or paclitaxel alone or in combination increased apoptosis in EAC cells in solid tumors.: Based on the indices of the early apoptosis marker of active caspase 3, a significant increase was observed in all treated groups compared to the control, as shown in Fig. 5A and 5B (P< 0.001). The combination group MNG 50mg/kg + PTX 12.5mg/kg was the most effective in increasing the active caspase 3 index (P< 0.001), as shown in Fig. 5A. Cleaved PARP results agreed with the active caspase 3 increased levels, as shown in Fig. 5B (P< 0.001). BAX protein levels increased only in the PTX group as compared with the control (P<0.001); however, in the groups that received MNG, a significant decrease was observed in both the single treatments and the combinations, as shown in Fig. 5A. It was observed that the number of late apoptotic cells (TUNEL) increased significantly in all treated groups compared to the control group, as shown in Fig. 5B (P<0.001). The apoptotic effect of the MNG 25mg/kg and 50mg/kg groups was higher than PTX 12.5mg/kg. In the combination groups, it was observed that the MNG 50mg/kg + PTX 12.5mg/kg group had the highest (P< 0.001) apoptotic index values compared to the control (Fig. 5).

Mangiferin, paclitaxel, and their combinations increased autophagy in EAC cells in solid tumors.: A significant increase in the LC3A levels was observed in the PTX 12.5mg/kg and MNG 50mg/kg + PTX 12.5mg/kg groups when compared to the control, as shown in Fig. 6A. However, compared with the control group, there was no significant difference in the MNG single groups except MNG 50mg/kg alone. LC3B reactions showed no significant difference between the MNG 100 mg/kg group and the control group. In all other groups, there was a significant increase (P<0.001) in LC3B levels compared with the control, as shown in Fig. 6A (P< 0.001). No significant differences between the groups that received MNG 100 mg/kg alone, PTX 12.5mg/kg alone, and MNG 10mg/kg + PTX 12.5mg/kg in combination were observed in the Atg5 levels compared to the control group. However, there was a significant increase in the Atg5 protein levels in MNG 25mg/kg, MNG 50mg/kg alone, and their combination groups compared to the control group, as shown in Fig. 6B (P<0.01; and P<0.001). Finally, p62 levels were significantly decreased (P<0.001) in all groups compared to the control. The lowest p62 levels were found in the MNG 50mg/kg + PTX 12.5mg/kg group, as shown in Fig. 6B.

Mangiferin, paclitaxel, and their combinations decreased p-AKT and increased PTEN expression in EAC solid tumors..: The p-AKT levels significantly decreased in all treated groups, as shown in Fig. 7 (P<0.001). A significant increase in PTEN levels was also observed in all treated groups (P<0.001) compared to the control group, except for the MNG 100mg/kg group, as

shown in Fig. 7. A decrease in p-AKT and an increase in PTEN levels suppressed survival in vivo in both the single and combination groups.

Mangiferin, paclitaxel, and their combinations suppressed angiogenesis in a CAM assay: According to the microscopic evaluation of CAM, as shown in Fig. 8 and Table 2, MNG 50µg/pellet and all groups showed a stronger antiangiogenic effect compared with the positive control thalidomide. In contrast, the MNG 25-12.5µg/pellet group showed a weak antiangiogenic effect. The antiangiogenic effect of PTX, whose antiangiogenic properties are well known, was investigated at decreasing doses using the CAM assay. Whereas 0.75-1.5- 3µg/pellet concentrations of PTX showed a very strong antiangiogenic effect (P< 0.001, P<0.01), the concentration of 0.375µg/pellet was found to have a strong antiangiogenic effect (Fig. 8, Table 2). This concentration of PTX that showed a strong effect was further combined with 50 µg/pellet, 25 µg/pellet, and 12.5 µg/pellet concentrations of MNG, and a very strong effect (P<0.05, P<0.001, P<0.001) was observed in all combinations as compared to the positive control (±) thalidomide, as shown in Fig. 8.

Table 2: Antiangiogenic effect results of Mangiferin, Paclitaxel alone and their combinations on CAM assay.

Drugs (mg/mL)	Concentration (µg/pellet)	Average score	Anti-angiogenic effect
(±)-Thalidomide (Positive control) 5	50	0.81±0.03	Strong effect
Agarose	2.5%, w/v	0.20±0.20	Inactive effect
MNG 5	50	0.96±0.09	Strong effect
MNG 2.5	25	0.72±0.10	Weak effect
MNG 1.25	12.5	0.66±0.11	Weak effect
PTX 0.3	3	1.80±0.08***	Very Strong effect
PTX 0.15	1.5	1.50±0.11**	Very Strong effect
PTX 0.075	0.75	1.11±0.09	Very Strong effect
PTX 0.0375	0.375	0.76±0.03	Strong effect
MNG 5 + PTX 0.0375	50+0.375	1.69±0.09***	Very Strong effect
MNG 2.5 + PTX 0.0375	25+0.375	1.46±0.10***	Very Strong effect
MNG 1,25 + PTX 0.0375	12.5+0.375	1.25±0.08*	Very Strong effect

*P<0.05 **P<0.01; ***P<0.001; significance values determined compared to the positive control (±) -thalidomide.

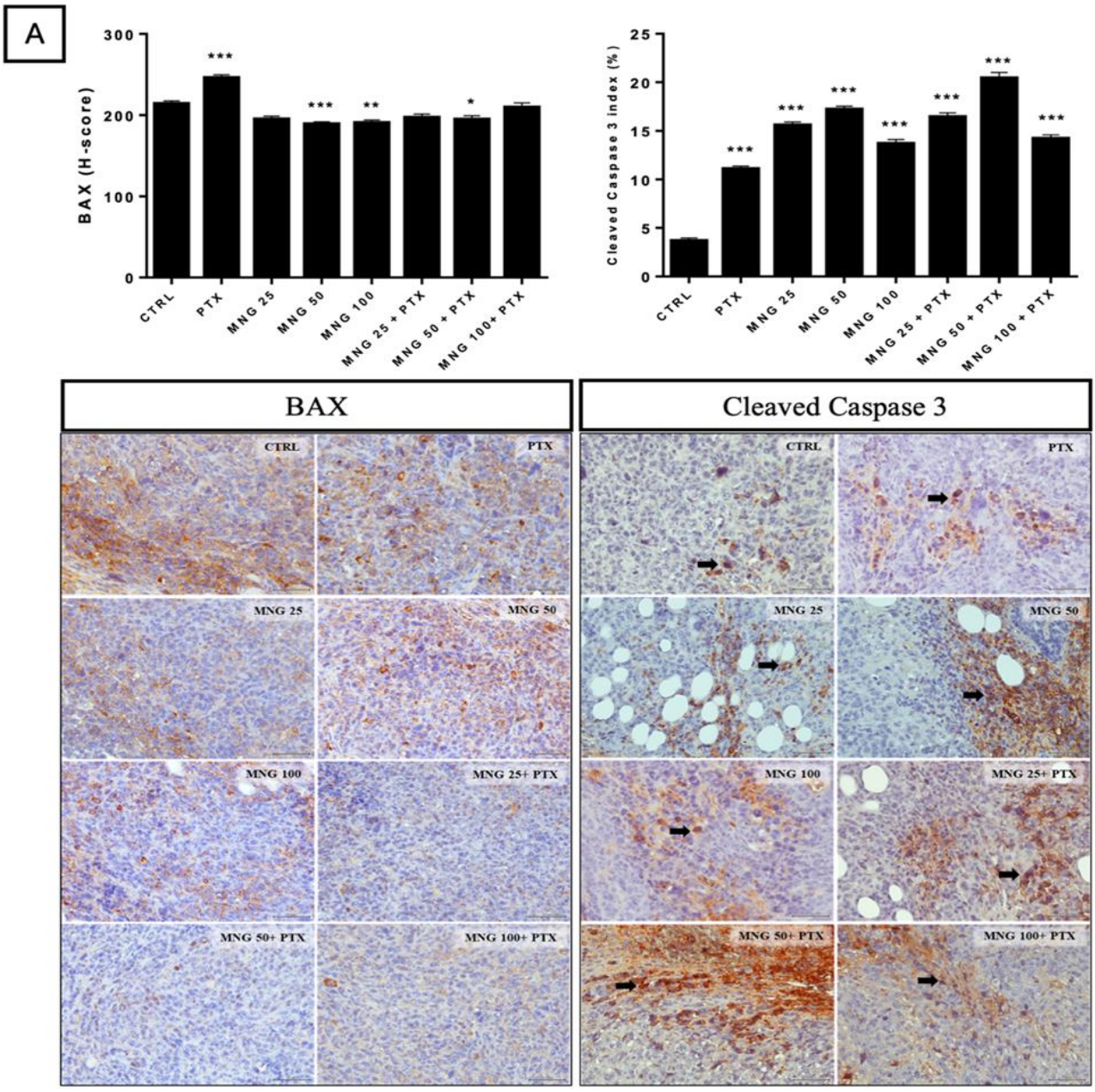

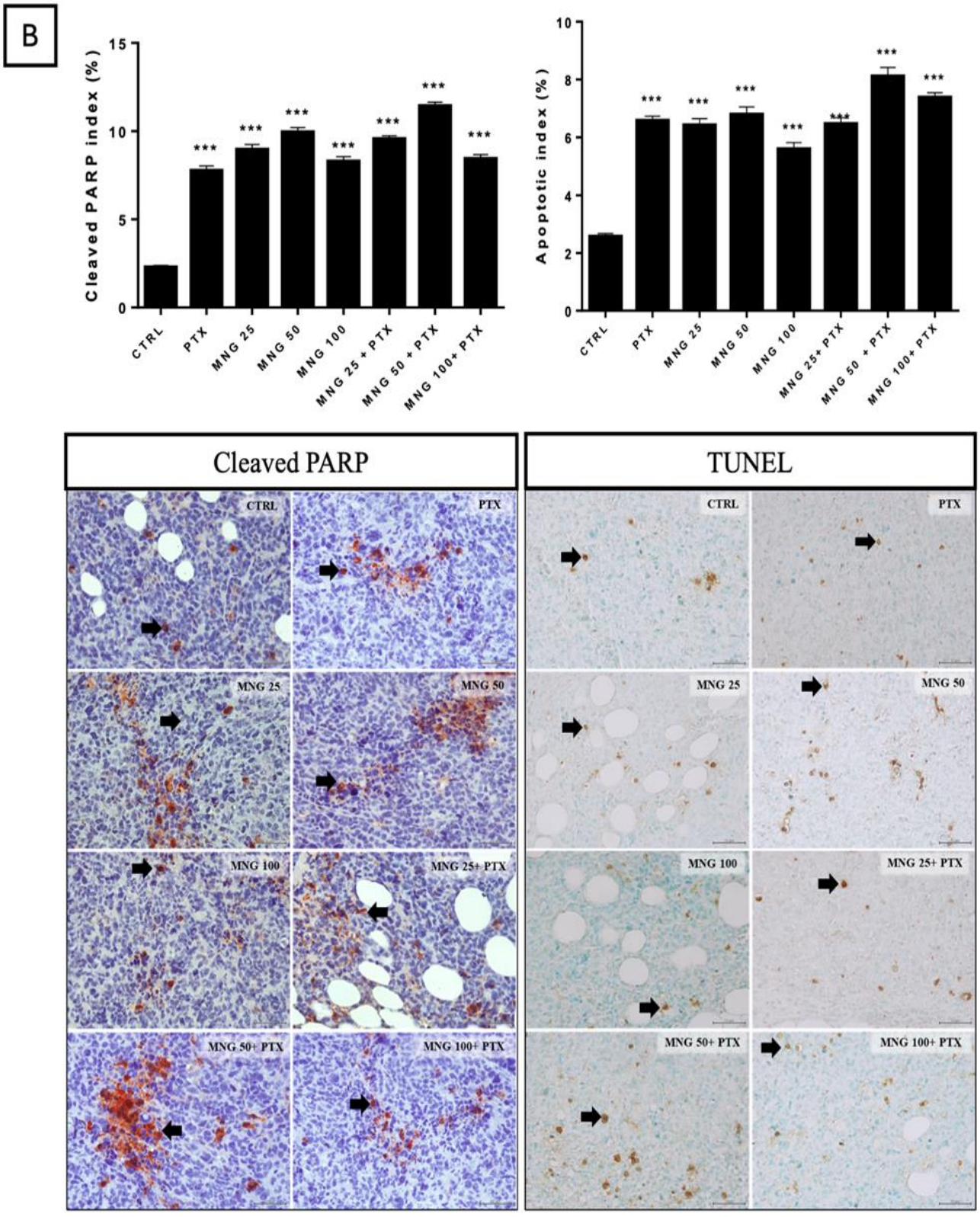

Fig. 5: **A**) BAX (H-score), cleaved caspase 3 index (%), **B**) cleaved PARP index (%), and apoptotic (TUNEL) index (%) graphics and their immunohistochemical micrograph. The effects of PTX (12.5mg/kg), MNG (25-50-100mg/kg) and their combination on apoptosis. Immunoreactivity is shown in nuclear (cleaved PARP and TUNEL), cytoplasmic (BAX and cleaved caspase 3) and red-brown or brown. Nuclear immunoreactivity are shown with an arrow (→),.*P<0.05, **P<0.01 and ***P<0.001, significance compared to the control group. Scale bars = 50μM (× 400).

DISCUSSION

MNG is a natural compound with potent anticancer activity that has been the focus of several studies. The study presented here investigated the effects of MNG, PTX, and their combinations on proliferation, apoptosis, autophagy, and survival pathways in EAC cells using *in vitro* and *in vivo* methods. The present study demonstrates that MNG potentiates the cytotoxic and pro-apoptotic effects of PTX, as well as enhancing its antiangiogenic capacity, thus suggesting a synergistic therapeutic interaction..

MNG has been shown to inhibit the growth of various cancer cell lines, but the effects are dependent on the cell type (Irshad *et al.*, 2024). In accordance with the findings of preceding studies, MNG demonstrated no evidence of toxicity towards normal endothelial cells (HUVECs), even at elevated concentrations, thereby substantiating its safety profile (Morozkina *et al.*, 2021). It is noteworthy that, in EAC cells, MNG alone exhibited limited toxicity; however, its combination with PTX resulted in a dose-dependent augmentation in cell death. This synergism is consistent with reports that MNG enhances the activity of standard chemotherapeutic agents, including platinum derivatives and doxorubicin (Rahmani *et al.*, 2023; Sarfraz *et al.*, 2023; Iqbal *et al.*, 2024; Irshad *et al.*, 2024; Melo-Betances *et al.*, 2025). In alignment with these findings, the current study observed that low doses of MNG (12.5–100µM) in HUVEC cells and high doses (300µM) in EAC cells acted synergistically with paclitaxel (PTX), resulting in increased cytotoxicity in a dose-dependent manner.

The present study demonstrated that both MNG and PTX effectively reduced EAC breast tumor volumes in vivo, with MNG at 50mg/kg, achieving the most significant reduction as a single-agent treatment. In the combination groups, the concentrations of MNG 25mg/kg and 50mg/kg exhibited a synergistic effect with PTX 12.5mg/kg,

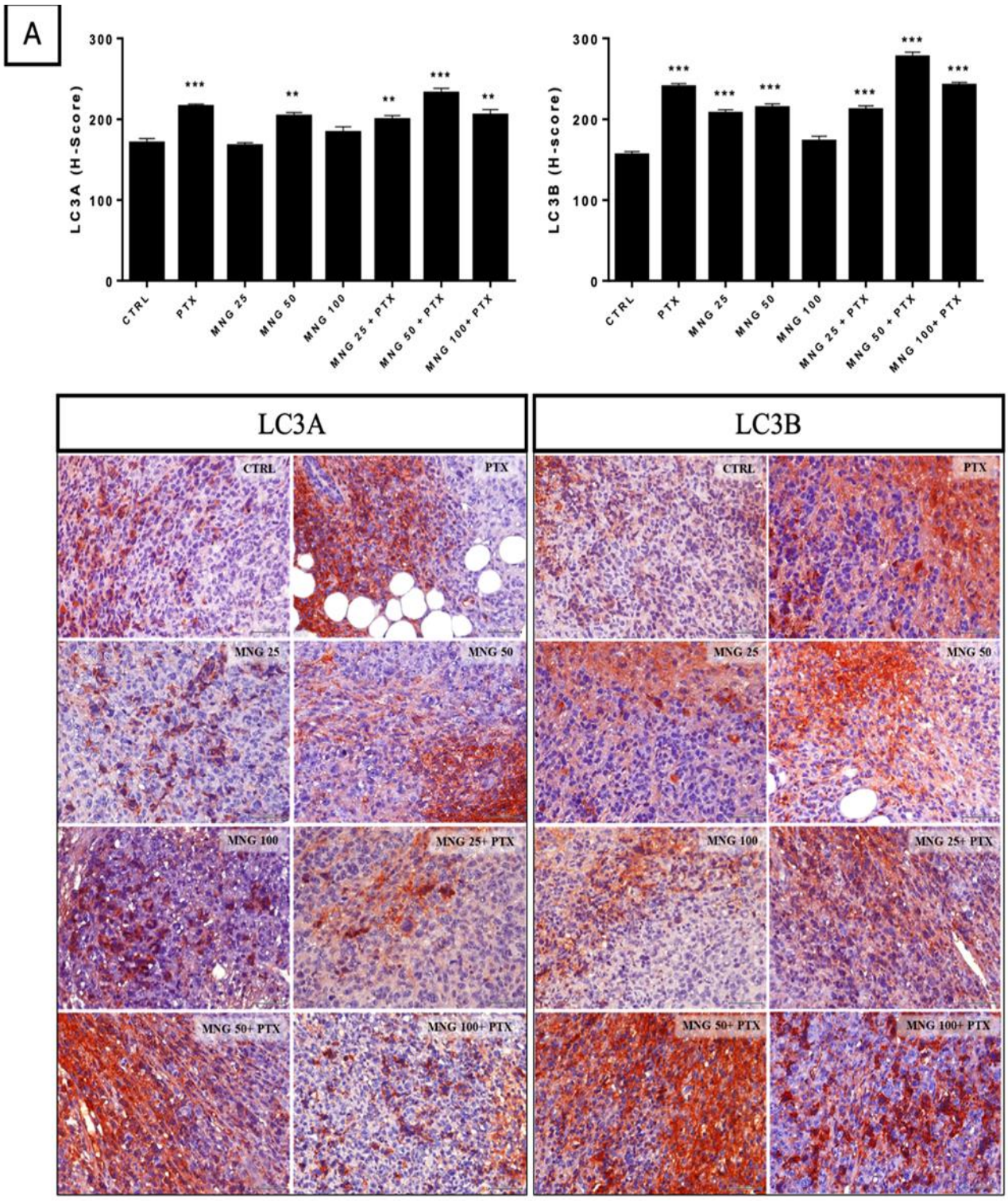

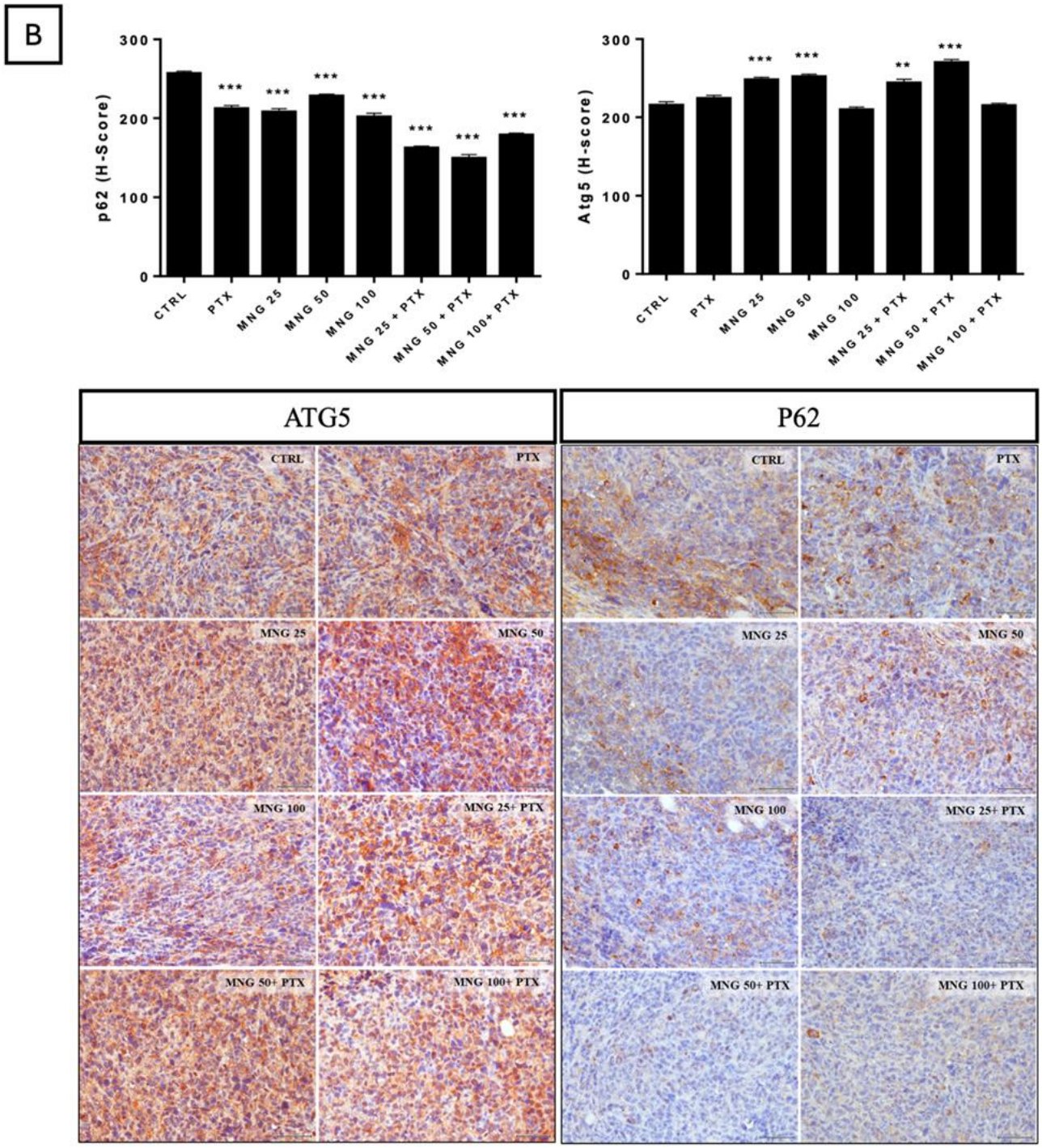

Fig. 6: A) LC3A (H-score), LC3B (H-score), **B)** ATG5 (H-score) and P62 (H-score) graphics and their immunohistochemical micrograph of EAC. The effect of PTX (12.5mg/kg), MNG (25-50-100mg/kg), and their combinations on autophagy. Immunoreactivity is cytoplasmic (LC3A, LC3B, ATG5 and P62) and red-brown or brown. **P<0.01 and ***P<0.001, significance compared to the control group. Scale bars = 50μM (× 400).

increasing tumor sensitivity and reducing tumor volumes by 65.48% and 71.70%, respectively. Consistent with the findings of this study, MNG at doses of 50 and 100mg/kg has been reported to reduce the tumor size in OVCAR3 and A549 cells by increasing sensitivity to cisplatin (Shi *et al.*, 2016; Zou *et al.*, 2017). In addition, Sadhukhan *et al.* (2018) further reported that MNG at 20mg/kg resulted in a significant reduction in EAC tumor volume, approaching almost 50% reduction. However, no synergistic effect was observed with cisplatin at 10mg/kg (Sadhukhan *et al.*, 2018). These results highlight the superior efficacy of the MNG and PTX combination in suppressing EAC tumor volume in comparison with cisplatin-based therapy, thereby emphasizing its potential as an effective therapeutic strategy.

Aberrant proliferation is an essential hallmark of cancer development. Consequently, the suppression of proliferation is one of the main goals of cancer treatment (Tong *et al.*, 2022). In a previous *In vivo* study, MNG 100mg/kg was reported to reduce Ki-67 and tumor volume (Li *et al.*, 2013) of MDA-MB-231 xenografts. Our study also observed that MNG at 25 and 50mg/kg reduced the

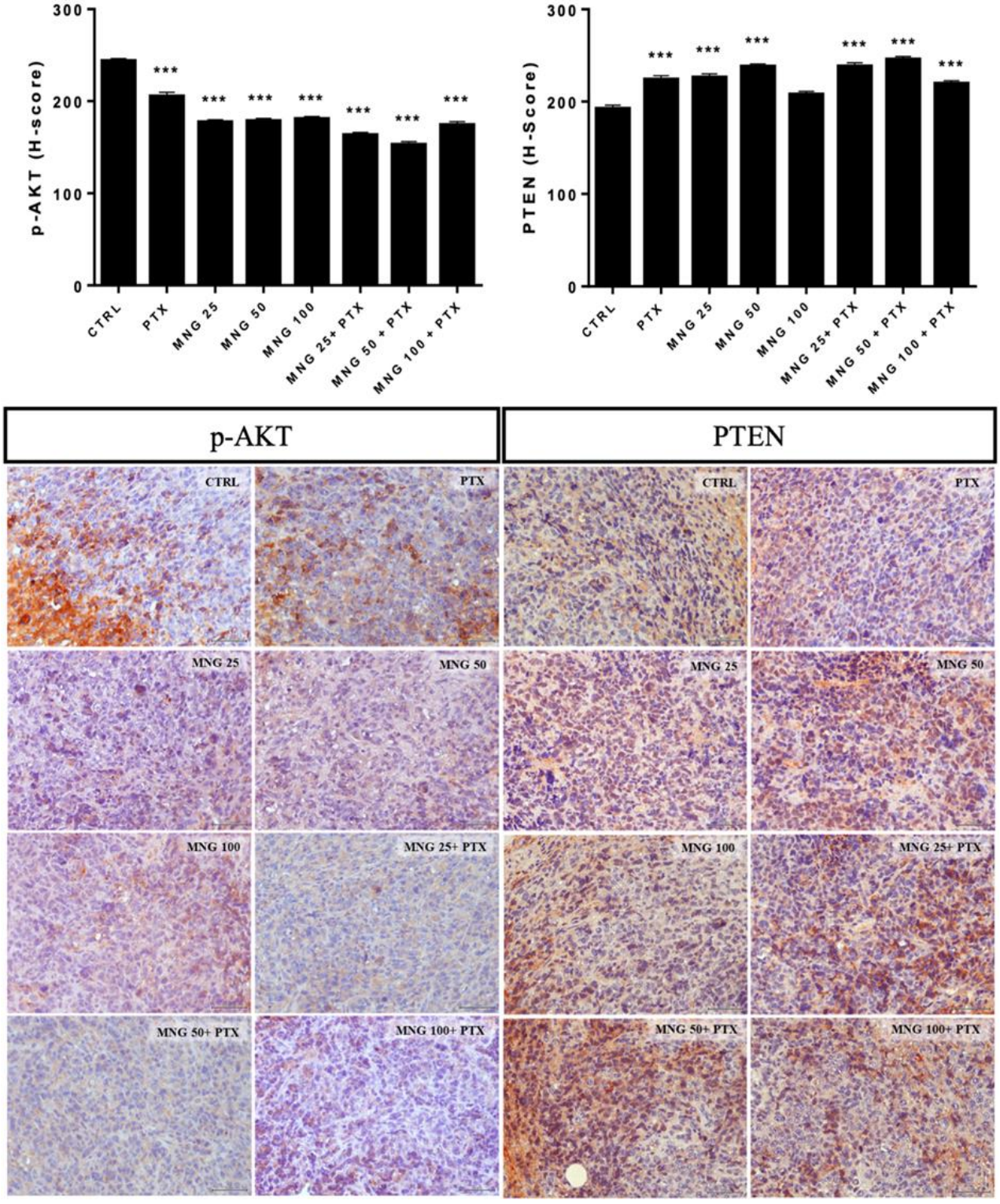

Fig. 7: p-AKT (H-score), PTEN (H-score) graphics and their immunohistochemical micrograph of EAC. The effect of PTX (12.5mg/kg), MNG (25-50-100mg/kg), and their combinations on intracellular signaling pathways. Immunoreactivity is cytoplasmic (p-AKT and PTEN) and red-brown or brown. ***P<0.001, significance compared to the control group. Scale bars = 50µM (× 400).

PCNA levels, and this reduction was in line with tumor volume. The study revealed a significant decrease in PCNA levels, with a 50.82% reduction observed in the MNG 50mg/kg group and a 38.81% decrease noted in the PTX 12.5mg/kg + MNG 50mg/kg group.

The suppression of apoptosis is a critical factor in cancer development, inducing apoptosis as a fundamental strategy in cancer treatment (Chaudhry *et al.*, 2022). MNG has been demonstrated to induce dose-dependent apoptosis in MCF7, MDA-MB-231, and OVCAR3 cancer cells. Its apoptotic effect in OVCAR3 is synergistically enhanced by cisplatin (1 µg/mL) (Li *et al.*, 2013; Zou *et al.*, 2017). In this study, the combination of MNG 300 µM and PTX 3.98 µM increased the level of FAS, suggesting an activation of the extrinsic apoptotic pathway (Peramaiyan Rajendran *et al.*, 2015). BAX, a marker of the intrinsic mitochondrial pathway, was found to be decreased in the co-treatment of MNG and PTX, both *in vitro* and *in vivo*.

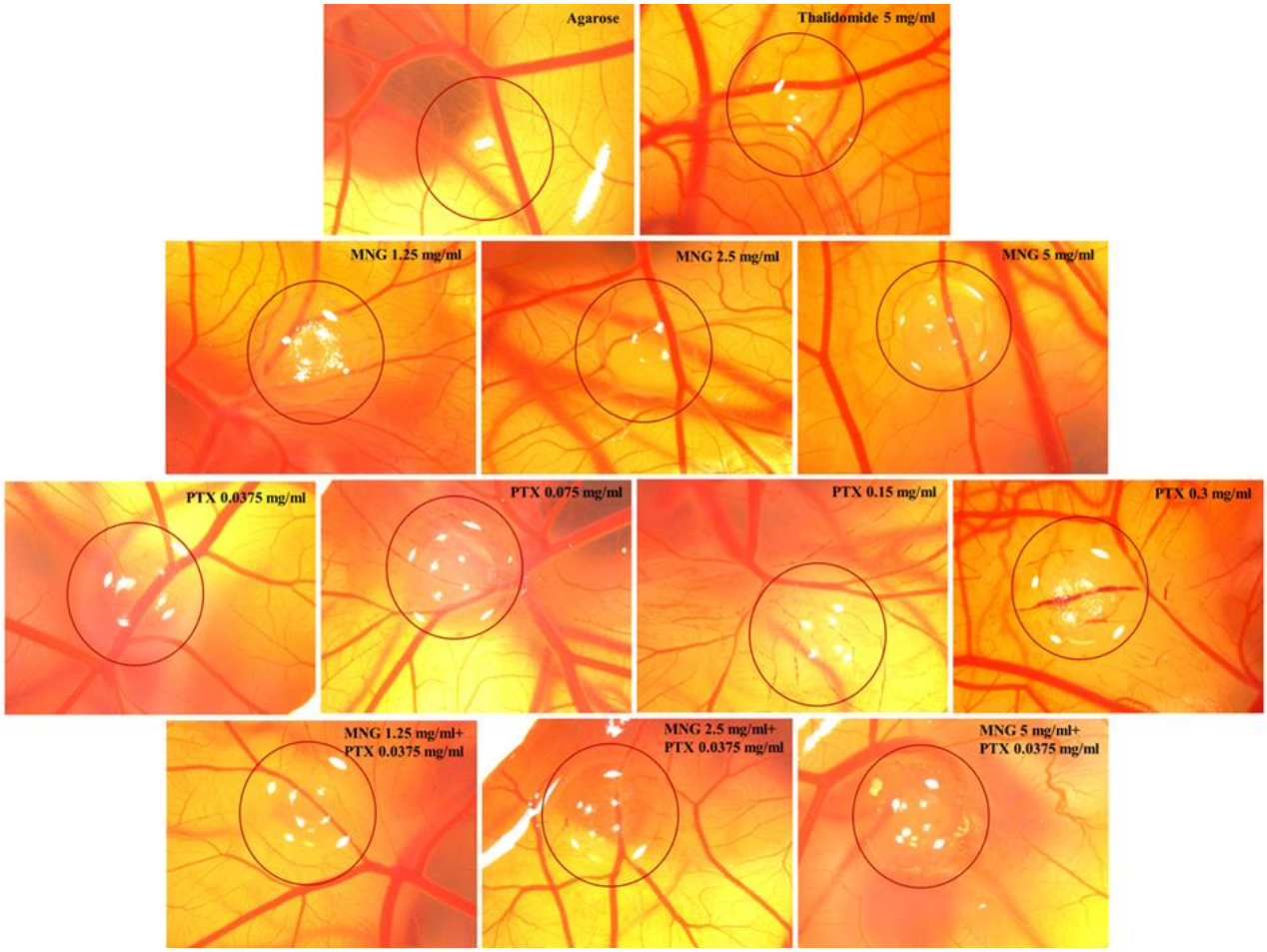

Fig. 8: The antiangiogenic effects of different concentrations of MNG, PTX and their combinations on branching blood vessels in the chick chorioallantoic membrane (CAM) test. The stereomicroscopic evaluation of MNG (1.25-5mg/mL), PTX (0.0375-0.3mg/mL), and PTX (0.0375mg/kg) in combination with MNG (1.25-5mg/mL) at CAM. Thalidomide and agarose were used as positive and negative controls, respectively.

Src phosphorylation modulates apoptosis by inactivating the proapoptotic genes Bad, BAX, and caspase-9 (Liu *et al.*, 2024). A significant increase in p-Src levels was observed in the combination groups, which was further associated with a substantial increase in cleaved PARP levels in EAC cells. PARP is cleaved during the process of apoptosis, which is a well-known hallmark of cellular suicide. The elevated levels of cleaved PARP indicate that the combination of MNG and PTX enhances apoptosis (Decker *et al.*, 2002). In the present study, an increase in p-Src, a decrease in BAX protein levels, and an increase in the expression of cleaved PARP were observed. The present findings suggest that p-Src can suppress BAX to bypass the mitochondrial pathway and induce apoptosis via the extrinsic pathway with an increase in FAS protein.

MNG increases active caspase-3 levels to promote apoptosis in various cancer cell lines (du Plessis-Stoman, du Preez, and van de Venter, 2011; Li *et al.*, 2016). Subsequent examination of the *in vivo* levels of active caspase-3 revealed an increase in all groups, thus indicating that the mode of cell death observed is that of apoptosis. The combination of MNG and PTX further increased active caspase-3 levels with a synergistic effect; besides, MNG 50mg/kg + PTX 12.5mg/kg was observed to have the highest active caspase-3 level. Moreover, the apoptotic cells in the late stage were examined by the TUNEL method, and an increase in apoptotic cell index was observed in all groups compared with the control. These results are consistent with the increased levels of active caspase-3 and cleaved PARP and the reduction in the PCNA levels and tumor volume. Taken together, the mechanism of cell death relies on apoptotic machinery activation.

In the previous studies, the effect of MNG at 100mg/kg on tumor volume and apoptosis was investigated (Rajendran, Ekambaram, and Sakthisekaran, 2008; Li *et al.*, 2013; Iqbal *et al.*, 2024).In the present study, the apoptotic effect in a dose-dependent manner using three different MNG doses was studied, with MNG 100mg/kg being weaker compared to the 50 and 25mg/kg doses. As with certain natural compounds, it conceivable that MNG may also exhibit dose-related antioxidant or prooxidant properties (Chobot and Hadacek, 2011; Martins *et al.*, 2014; Dzah *et al.*, 2024). The findings of this study indicate that MNG 50mg/kg is the optimal effective concentration on EAC tumors.

In addition to apoptosis, autophagy is an essential process that aids in eliminating cancer cells (Su *et al.*, 2013). The relationship between autophagy and apoptosis is frequently characterised as intricate. Autophagy can be considered as either a facilitator of cell death or a promoter of cell survival, depending on the cellular context (Eisenberg-Lerner *et al.*, 2009; Z. Wu *et al.*, 2024; Kouri *et al.*, 2025). The in vitro results demonstrate that the combination of PTX and MNG increases the proteins p-Beclin, Atg5, LC3A, and LC3B in EAC cells. This finding

indicates that the process of autophagy is underway and nearing completion (Hizomi Arani *et al.*, 2022). In line with these studies, the in vivo results showed a significant increase in Atg5, LC3A, and LC3B with a substantial decrease in p62 in the co-treatment groups, which aligns with the in vivo results.

When autophagy is excessively activated, it can lead to autophagic cell death, which may also result in PARP cleavage, albeit through different pathways (Wang *et al.*, 2014; Zhang *et al.*, 2022). The activation of autophagy through Beclin1 has been shown to promote apoptosis in cancer cells, particularly when combined with chemotherapeutic agents (Sun *et al.*, 2010). The promotion of autophagy alongside apoptosis is evidenced by the increased expression of Beclin 1 and LC3β/LC3α in cancer cells (Yu *et al.*, 2019; Lin *et al.*, 2020). In the present study, the decrease in p62 with a concomitant increase in Atg5 and LC3B indicates an increase in autophagy. In contrast, the decreased tumor volume and increased apoptosis suggest that MNG and PTX co-treatment not only triggers apoptosis but also promotes autophagy, which may act as a complementary cell death mechanism. The balance between apoptosis and autophagy likely contributes to the enhanced cytotoxicity observed in both experimental settings (Kumar *et al.*, 2015; Kouri *et al.*, 2025).

PTEN, the tumor suppressor gene, suppresses AKT phosphorylation (Peacock *et al.*, 2009; Park *et al.*, 2019). MNG modulated the PI3K/AKT pathway, reducing cell viability in gastric cancer and OVCAR3 cells dose-dependently (Zou *et al.*, 2017; Du *et al.*, 2018). Similarly, the combination of PTX and MNG decreased p-AKT expression and a slight increase in PTEN expression in vitro and in vivo. Increasing PTEN expression enhances FAS/FASL-mediated apoptosis (Peacock *et al.*, 2009). Notably, FAS was also significantly increased in this study, as reported above. Also, MNG suppresses ERK and JNK signaling pathways (Xie *et al.*, 2025). Our study also observed that the in vitro expression of p-c-Jun decreased in the PTX and MNG combination, which is a downstream protein of the JNK signaling pathway. All these data suggest that the co-treatment of PTX and MNG might suppress cell survival signaling and trigger cell death in vitro and in vivo in EAC cells.

Angiogenesis is crucial to tumor progression, making it a key target in cancer therapy (Folkman, 2007; Yang *et al.*, 2025). While research on the antiangiogenic effects of MNG is limited, one in vitro study demonstrated dose-dependent inhibitory effects of MNG on the tube-forming ability of EA.hy926 endothelial cells (Delgado-Hernández *et al.*, 2020). Our results show that low-dose combinations of MNG and PTX are sufficient for interrupting tube structures, indicating an antiangiogenic effect in vitro.

Delgado-Hernández *et al.* (2020) reported that vascularization was suppressed when MNG was applied at a concentration of 50µg/disk to the CAM area, with increased vascularization by bFGF (Delgado-Hernández *et al.*, 2020). In this study, MNG also showed a strong antiangiogenic effect at a concentration of 5mg/mL (50µg/pellet). The combination of low-dose PTX and MNG at concentrations of 5-2.5-1.25mg/mL had a stronger antiangiogenic effect than single treatments in the CAM assay. The low-dose PTX and MNG combination had a very strong antiangiogenic effect in the CAM model, which is similar to the results seen in in vitro. MNG has been shown to enhance the antiangiogenic effect of PTX, even at low concentrations, which represents a significant advancement in cancer treatment. Both in vitro tube formation and in vivo CAM assays revealed that MNG, especially in combination with low-dose PTX, markedly inhibited neovascularization

Conclusions: In conclusion, this study provides substantial evidence that mangiferin significantly enhances the antitumour efficacy of paclitaxel through complementary mechanisms involving the induction of apoptosis, the activation of autophagy, and the inhibition of angiogenesis. The MNG and PTX combination was found to have a synergistic effect, resulting in marked tumor regression in vivo and pronounced cytotoxicity in vitro without affecting normal endothelial cells, which emphasizes its potential safety and selectivity.

At a molecular level, MNG appears to make cancer cells more sensitive to paclitaxel by modulating multiple signaling cascades, including the PI3K/AKT, JNK and Src pathways. This leads to the upregulation of proapoptotic markers (FAS, cleaved PARP and caspase-3) and the suppression of markers associated with proliferation and survival (PCNA, p-AKT and p-c-Jun). Additionally, the concurrent activation of autophagic processes suggests a cooperative interplay between apoptosis and autophagy in MNG-mediated cell death.

From a therapeutic perspective, these findings suggest that MNG could be used as an effective adjuvant in chemotherapy regimens. Its ability to increase the efficacy of paclitaxel at lower doses could reduce the adverse side effects commonly associated with conventional chemotherapy, thereby improving patient outcomes. Future studies should aim to elucidate the pharmacokinetic interactions of MNG and PTX, as well as evaluate their effects in other tumor models and clinical settings. Furthermore, exploring the nanoformulation or targeted delivery of MNG could enhance its bioavailability and applicability in clinical settings.

Overall, this work highlights mangiferin's potential as a natural, safe and effective chemosensitiser that could strengthen the therapeutic potential of paclitaxel, paving the way for its use in future anticancer strategies.

Acknowledgments: The authors especially thank Mudurnu Piliç- Pak Tavuk Company for providing fertilized hen eggs. None of the authors has a commercial interest, financial interest, and/or other relationship with manufacturers of pharmaceuticals, laboratory supplies, and/or medical devices or with commercial providers of medical services.

Funding: The Research Fund of Istanbul University-Cerrahpasa supported the present work. Project No. TDK-2017-26107.

Data availability: All data generated and/or analyzed during this study are available from the corresponding authors upon reasonable request.

Ethics approval and consent to participate: The *in vivo* solid tumor model protocol was approved by the Animal Welfare and Use Committee of Istanbul University (No: 141199/12.04.2017).

Conflict of interest: The authors declare that they have no competing interests.

Authors contribution: Ayca Uvez: Designed and performed the experiments and analyzed the data, investigation Writing-Review & Editing. Engin Ulukaya Designed and performed the experiments and Analyzed and interpreted the data, Investigation, Writing-Review & Editing . Elif Ilkay Armutak: Designed and performed the experiments and Analyzed and interpreted the data, Investigation, Writing-Review&Editing. All authors approved the final version of the manuscript.

REFERENCES

Aboyewa JA, Sibuyi NRS, Meyer M, *et al*., 2021. Gold nanoparticles synthesized using extracts of cyclopia intermedia, commonly known as honeybush, amplify the cytotoxic effects of doxorubicin. Nanomaterials 11:132.

Adiyeke E, Bakan N, Uvez A, *et al*., 2024. The effect of N-acetylcysteine on the neurotoxicity of sevoflurane in developing hippocampus cells. Neurotoxicology 103:96–104.

Aydinlik S, Uvez A, Kiyan HT, *et al*., 2021. Palladium (II) complex and thalidomide intercept angiogenic signaling via targeting FAK/Src and Erk/Akt/PLCγ dependent autophagy pathways in human umbilical vein endothelial cells. Microvascular Research 138:104229.

Chaudhry GES, Md Akim A, Sung YY, *et al*., 2022. Cancer and apoptosis: The apoptotic activity of plant and marine natural products and their potential as targeted cancer therapeutics. Front Pharmacol 13.

Chobot V and Hadacek F, 2011. Exploration of pro-oxidant and antioxidant activities of the flavonoid myricetin. Redox Report 16:242–247.

Decker P and Muller S, 2002. Modulating Poly (ADP-Ribose) Polymerase Activity: Potential for the prevention and therapy of pathogenic situations involving DNA damage and oxidative stress. Current Pharmaceutical Biotechnology 3:275–283.

Delgado-Hernández R, Hernández-Balmaseda I, Rodeiro-Guerra I, *et al*., 2020. Anti-angiogenic effects of mangiferin and mechanism of action in metastatic melanoma. Melanoma Research 30:39–51.

Du M, Wen G, Jin J, *et al*., 2018. Mangiferin prevents the growth of gastric carcinoma by blocking the PI3K-Akt signalling pathway. Anticancer Drugs 29:167–175.

Dutta T, Das T, Gopalakrishnan AV, *et al*., 2023. Mangiferin: the miraculous xanthone with diverse pharmacological properties. Naunyn-Schmiedeberg's Archives of Pharmacology 396:851–863.

Dzah CS, Zhang H, Gobe V, *et al*., 2024. Anti- and pro-oxidant properties of polyphenols and their role in modulating glutathione synthesis, activity and cellular redox potential: Potential synergies for disease management. Advances in Redox Research 11:100099.

Eisenberg-Lerner A, Bialik S, Simon HU, *et al*., 2009. Life and death partners: apoptosis, autophagy and the cross-talk between them. Cell Death & Differentiation 16:966–975.

Folkman J, 2007. Angiogenesis: an organizing principle for drug discovery? Nat Rev Drug Discov 6:273–286.

He W, You Y, Du S, *et al*., 2018. Anti-neoplastic effect of mangiferin on human ovarian adenocarcinoma OVCAR8 cells via the regulation of YAP. Oncology Letters 17.

Hizomi Arani R, Mohammadpour H, Moosavi MA, *et al*., 2022. The role of autophagy-related proteins of Beclin-1/BECN1, LC3II, and p62/SQSTM1 in melanoma tumors. Asian Pacific Journal of Cancer Biology 6:263–272.

Ikitimur-Armutak EI, Sonmez K, Akgun-Dar K, *et al*., 2015. Anticancer effect of a novel palladium-saccharinate complex of terpyridine by inducing apoptosis on Ehrlich ascites carcinoma (EAC) in Balb-C mice. Anticancer Research 35:1491–1497.

Iqbal H, Inam-Ur-Raheem M, Munir S, *et al*., 2024. Therapeutic potential of mangiferin in cancer: Unveiling regulatory pathways, mechanisms of action, and bioavailability enhancements – An updated review. Food Science & Nutrition 12.

Irshad N, Naeem H, Shahbaz M, *et al*., 2024. Mangiferin: An effective agent against human malignancies. Food Science & Nutrition 12:7137–7157.

Jiang X, 2025. The pharmacology of paclitaxel in cancer therapy. BIO Web of Conferences 166:02002.

Kouri MA, Tsaroucha A, Axakali T-M, *et al*., 2025. Targeting cancer cell fate: apoptosis, autophagy, and gold nanoparticles in treatment strategies. Current Issues in Molecular Biology 47:460.

Krenn L and Paper DH, 2009. Inhibition of angiogenesis and inflammation by an extract of red clover (Trifolium pratense L.). Phytomedicine 16:1083–1088.

Kumar D, Das B, Sen R, *et al*., 2015. Andrographolide analogue induces apoptosis and autophagy mediated cell death in U937 cells by inhibition of PI3K/Akt/mTOR pathway. PLoS One 10:e0139657.

Li H, Huang J, Yang B, *et al*., 2013. Mangiferin exerts antitumor activity in breast cancer cells by regulating matrix metalloproteinases, epithelial to mesenchymal transition, and β-catenin signaling pathway. Toxicology and Applied Pharmacology 272:180–190.

Lin Y, Tsai K, Chen J, *et al*., 2020. Mangiferin inhibits lipopolysaccharide-induced epithelial-mesenchymal transition (<scp>EMT</scp>) and enhances the expression of tumor suppressor gene *PER1* in non-small cell lung cancer cells. Environmental Toxicology 35:1070–1081.

Liu R, Ouyang J and Li L, 2024. Anti-tumor activity of beauvericin: focus on intracellular signaling pathways. Mycotoxin Res 40:535–546.

LI M, MA H, YANG L, *et al*., 2016. Mangiferin inhibition of proliferation and induction of apoptosis in human prostate cancer cells is correlated with downregulation of B-cell lymphoma-2 and upregulation of microRNA-182. Oncology Letters 11:817–822.

Martins LAM, Coelho BP, Behr G, *et al*., 2014. Resveratrol induces pro-oxidant effects and time-dependent resistance to cytotoxicity in activated hepatic stellate cells. Cell Biochem Biophys 68:247–257.

Mei S, Ma H and Chen X, 2021. Anticancer and anti-inflammatory properties of mangiferin: A review of its molecular mechanisms. Food and Chemical Toxicology 149:111997.

Melo-Betances E, Rodríguez-Bautista CC and Núñez-Sellés AJ, 2025. Synthesis of mangiferin derivatives, complexes, and carriers as potential therapeutic candidates for cancer treatment: an update. Frontiers in Pharmacology 16:1598719.

Morozkina SN, Nhung Vu TH, Generalova YE, *et al*., 2021. Mangiferin as new potential anti-cancer agent and mangiferin-integrated polymer systems-a novel research direction. Biomolecules 11.

Park MK, Yao Y, Xia W, *et al*., 2019. PTEN self-regulates through USP11 via the PI3K-FOXO pathway to stabilize tumor suppression. Nature Communications 10:636.

Peacock JW, Palmer J, Fink D, *et al*., 2009. PTEN loss promotes mitochondrially dependent type ıı fas-ınduced apoptosis via PEA-15. Molecular and Cellular Biology 29:1222–1234.

du Plessis-Stoman D, du Preez J and van de Venter M, 2011. Combination treatment with oxaliplatin and mangiferin causes increased apoptosis and downregulation of NFκB in cancer cell lines. African Journal of Traditional, Complementary and Alternative Medicines 8:177–184.

Radulski DR, Stipp MC, Galindo CM, *et al*., 2023. Features and applications of Ehrlich tumor model in cancer studies: a literature review. Translational Breast Cancer Research 4:22.

Rahmani AH, Almatroudi A, Allemailem KS, *et al*., 2023. Role of mangiferin in management of cancers through modulation of signal transduction pathways. Biomedicines 11.

Rajendran P, Ekambaram G and Sakthisekaran D, 2008. Effect of mangiferin on benzo(a)pyrene induced lung carcinogenesis in experimental Swiss albino mice. Natural Product Research 22:672–680.

Rajendran P, Rengarajan T, Nandakumar N, *et al*., 2015. Mangiferin in cancer chemoprevention and treatment: pharmacokinetics and molecular targets. Journal of Receptors and Signal Transduction 35:76–84.

Rodriguez-Gonzalez JC, Hernández-Balmaseda I, Declerck K, *et al*., 2021. Antiproliferative, antiangiogenic, and antimetastatic therapy response by mangiferin in a syngeneic ımmunocompetent colorectal cancer mouse model ınvolves changes in mitochondrial energy metabolism. Frontiers in Pharmacology 12.670167

Sadhukhan P, Saha S, Dutta S, *et al*., 2018. Mangiferin ameliorates cisplatin ınduced acute kidney ınjury by upregulating Nrf-2 via the activation of PI3K and exhibits synergistic anticancer activity with cisplatin. Frontiers in Pharmacology 9:638.

Sarfraz M, Khan A, Batiha GES, *et al*., 2023. Nanotechnology-based drug delivery approaches of mangiferin: promises, reality and challenges in cancer chemotherapy. Cancers (Basel) 15.16:4194

Shi W, Deng J, Tong R, *et al.*, 2016. Molecular mechanisms underlying mangiferin-induced apoptosis and cell cycle arrest in A549 human lung carcinoma cells. Molecular Medicine Reports 13:3423–3432.

Su M, Mei Y and Sinha S, 2013. Role of the crosstalk between autophagy and apoptosis in cancer. Journal of Oncology 2013:1–14.

Sun Y, Liu J, Jin L, *et al.*, 2010. Over-expression of the Beclin1 gene upregulates chemosensitivity to anti-cancer drugs by enhancing therapy-induced apoptosis in cervix squamous carcinoma CaSki cells. Cancer Letters 294:204–210.

Tong X, Tang R, Xiao M, *et al*., 2022. Targeting cell death pathways for cancer therapy: recent developments in necroptosis, pyroptosis, ferroptosis, and cuproptosis research. Journal of Hematology & Oncology 15:174.

Uvez A, Aydinlik S, Esener OBB, *et al*., 2020. Synergistic interactions between resveratrol and doxorubicin inhibit angiogenesis both *In vitro* and *In vivo*. Polish Journal of Veterinary Sciences 23:571–580.

Uvez A, Kılıc S, Esener OBB, *et al*., 2021. Combinatorial usage of sumac unriped fruit extract (*rhus coriaria*) and tannic acid enhanced synergistic anti-angiogenic effect on chick chorioallantoic membrane assay. Acta Veterinaria Eurasia 47:2–9.

Wang B, Shen J, Wang Z, *et al*., 2018. Isomangiferin, a novel potent vascular endothelial growth factor receptor 2 kinase ınhibitor, suppresses breast cancer growth, metastasis and angiogenesis. Journal of Breast Cancer 21:11.

Wang Y, Kuramitsu Y, Tokuda K, *et al*., 2014. Gemcitabine ınduces poly (ADP-Ribose) Polymerase-1 (PARP-1) degradation through autophagy in pancreatic cancer. PLoS One 9:e109076.

Wu J, Li Y, He Q, *et al*., 2023. Exploration of the use of natural compounds in combination with chemotherapy drugs for tumor treatment. Molecules 28:1022.

Wu Z, Cui Y, Mao W, *et al.*, 2024. Bufalin promotes apoptosis and autophagy through the jak-stat signaling pathway in myeloid leukemia. Pakistan Veterinary Journal 44:1142–1152.

Xie C, Hu M and Niu B, 2025. Mangiferin can alleviate atopic dermatitis-like responses in mice and HaCaT cells. Molecular & Cellular Toxicology 21:755–768.

Yang S, Fang Y, Ma Y, *et al*., 2025. Angiogenesis and targeted therapy in the tumour microenvironment: From basic to clinical practice. Clinical and Translational Medicine 15:e70313.

Yap KM, Sekar M, Seow LJ, *et al*., 2021. Mangifera indica (Mango): A promising medicinal plant for breast cancer therapy and understanding ıts potential mechanisms of action. Breast cancer (Dove Medical Press)13:471–503.

Yu L, Chen M, Zhang R, *et al*., 2019. Inhibition of cancer cell growth in gemcitabine-resistant pancreatic carcinoma by mangiferin phytochemical involves induction of autophagy, endogenous ROS production, cell cycle disruption, mitochondrial mediated apoptosis and suppression of cancer cell migration and invasion. Journal of Balkan Union of Oncology 24:1581–1586.

Zhang D, Lai W, Liu Y, *et al*., 2022. Chaperone-mediated autophagy attenuates H_2O_2-induced cardiomyocyte apoptosis by targeting poly (ADP-ribose) polymerase 1 (PARP1) for lysosomal degradation. Cell Biology International 46:1915–1926.

Zou B, Wang H, Liu Y, *et al*., 2017. Mangiferin induces apoptosis in human ovarian adenocarcinoma OVCAR3 cells via the regulation of Notch3. Oncology Reports 38:1431–1441.